Rearrangement and Dissociative Reactions of the Methanol Radical Cation ($CH_3OH^{\cdot+}$): A Comparison of Theory and Experiment

Ngai Ling Ma,[1a] Brian J. Smith,[1a] John A. Pople,[1a,b] and Leo Radom*,[1a]

Contribution from the Research School of Chemistry, Australian National University, Canberra, A.C.T. 2601, Australia, and Department of Chemistry, Carnegie-Mellon University, Pittsburgh, Pennsylvania 15213. *Received February 20, 1991*

Abstract: Ab initio molecular orbital theory at the G1 and G2 levels has been used to examine in detail the rearrangement and dissociative reactions of ionized methanol. The G2 calculations perform slightly but consistently better than G1. Theoretical (G2) and experimental relative energies are found generally to agree to within 0.1 eV for stable structures and 0.15 eV for transition structures (a total of 31 comparisons). The G2 calculations provide new estimates of the energy differences (at 0 K) between $CH_3OH^{\cdot+}$ and its distonic isomer $CH_2OH_2^{\cdot+}$ (-32 kJ mol^{-1}), between $CH_2O^{\cdot+}$ and $HCOH^{\cdot+}$ (+25 kJ mol^{-1}), and between HCO^+ and COH^+ (+156 kJ mol^{-1}). The present calculations support a recently reported value of 968 kJ mol^{-1} for $\Delta H_f°_{298}$ of $HCOH^{\cdot+}$ and suggest a value of 983 kJ mol^{-1} for $\Delta H_f°_{298}$ of COH^+. Four separate pathways for fragmentation of $CH_3OH^{\cdot+}$ to give HCO^+ have been characterized, with calculated energy requirements in striking agreement with experimental appearance energies. An ion-neutral complex ($CH_2OH\cdots H^{\cdot+}$) is found to play an important role in the lowest energy pathway for production of $CH_2O^{\cdot+}$ from $CH_2OH_2^{\cdot+}$.

Introduction

The methanol radical cation ($CH_3OH^{\cdot+}$) and its rearrangement and fragmentation products are fundamental species in organic mass spectrometry. The main possible rearrangement product is the methyleneoxonium radical cation ($CH_2OH_2^{\cdot+}$), a prototype distonic radical cation, while the possible dissociation products include hydroxymethyl cation (CH_2OH^+), formaldehyde radical cation ($CH_2O^{\cdot+}$), hydroxymethylene radical cation ($HCOH^{\cdot+}$), formyl cation (HCO^+), isoformyl cation (COH^+), and carbon monoxide cation ($CO^{\cdot+}$). There have been extensive experimental studies of these species, and considerable thermochemical information has been accumulated.[2-21]

On the theoretical side, there have been a number of detailed studies of various aspects of the potential energy surfaces associated with the species above.[9,13,21-31] However, a treatment of the overall surface at a uniform level of theory has yet to be reported, and several of the rearrangement and dissociation processes have not been investigated at all. Such a uniform treatment is one of the aims of the present study.

A second goal is to provide further assessment of the Gaussian-1 (G1)[32] and Gaussian-2 (G2)[33] levels of theory, recently introduced by Pople and co-workers with the aim of allowing widespread determination of molecular thermochemical information to useful quantitative accuracy. Such G1 and G2 calculations have been able to reproduce atomization energies, ionization energies, electron affinities, and proton affinities for a wide selection of molecules containing first- and second-row atoms to within 0.1 eV (10 kJ mol^{-1}) in most cases. The tests of G1 and G2 theory to date have been restricted to energy comparisons involving stable species.[32-34] This is extended in the present paper to comparisons involving transition structures, utilizing experimental appearance energy values for comparison with calculated activation energies.

Methods and Results

Standard ab initio molecular orbital calculations[35] at the G1 and G2 levels of theory[32,33] were carried out by using the GAUSSIAN 86,[36] GAUS-

(1) (a) Australian National University. (b) Permanent address: Carnegie-Mellon University.
(2) Lias, S. G.; Bartmess, J. E.; Liebman, J. F.; Holmes, J. L.; Levin, R. D.; Mallard, W. G. *J. Phys. Chem. Ref. Data, Suppl.* **1988**, *17*.
(3) Momigny, J.; Wankenne, H.; Krier, C. *Int. J. Mass Spectrom. Ion Phys.* **1980**, *35*, 151.
(4) Refaey, K. M. A.; Chupka, W. A. *J. Chem. Phys.* **1968**, *48*, 5205.
(5) Lifshitz, C.; Shapiro, M.; Sternberg, R. *Isr. J. Chem.* **1969**, *7*, 391.
(6) Warneck, P. *Z. Naturforsch.* **1971**, *26A*, 2047.
(7) Berkowitz, J. *J. Chem. Phys.* **1978**, *69*, 3044.
(8) Traeger, J. C. *Int. J. Mass Spectrom. Ion Processes* **1985**, *66*, 271.
(9) Ma, N. L.; Smith, B. J.; Collins, M. A.; Pople, J. A.; Radom, L. *J. Phys. Chem.* **1989**, *93*, 7759.
(10) Burgers, P. C.; Mommers, A. A.; Holmes, J. L. *J. Am. Chem. Soc.* **1983**, *105*, 5976.
(11) Harland, P. W.; Kim, N. D.; Petrie, S. A. H. *Aust. J. Chem.* **1989**, *42*, 9.
(12) Burgers, P. C.; Holmes, J. L. *Chem. Phys. Lett.* **1983**, *97*, 236.
(13) Wijenberg, J. H. O. J.; Van Lenthe, J. H.; Ruttink, P. J. A.; Holmes, J. L.; Burgers, P. C. *Int. J. Mass Spectrom. Ion Processes* **1987**, *77*, 141.
(14) Freeman, C. G.; Knight, J. S.; Love, J. G.; McEwan, M. J. *Int. J. Mass Spectrom. Ion Processes* **1987**, *80*, 255.
(15) Guyon, P. M.; Chupka, W. A.; Berkowitz, J. *J. Chem. Phys.* **1976**, *64*, 1419.
(16) Matthews, C. S.; Warneck, P. *J. Chem. Phys.* **1969**, *51*, 854.
(17) Baker, A. D.; Baker, C.; Brundle, C. R.; Turner, D. W. *Int. J. Mass Spectrom. Ion Phys.* **1968**, *1*, 285.
(18) Wankenne, H.; Caprace, G.; Momigny, J. *Int. J. Mass Spectrom. Ion Processes* **1984**, *57*, 149.
(19) Dyke, J. M.; Jonathan, N. B. H.; Morris, A.; Winter, M. J. *Mol. Phys.* **1980**, *39*, 629.
(20) McMahon, T. B.; Kebarle, P. *J. Chem. Phys.* **1985**, *83*, 3919.
(21) Bouma, W. J.; Burgers, P. C.; Holmes, J. L.; Radom, L. *J. Am. Chem. Soc.* **1986**, *108*, 1767.
(22) Bouchoux, G. *Mass Spectrom. Rev.* **1988**, *7*, 1.
(23) DeFrees, D. J.; McLean, A. D.; Herbst, E. *Astrophys. J.* **1984**, *279*, 322.
(24) Bouma, W. J.; Nobes, R. H.; Radom, L. *J. Am. Chem. Soc.* **1982**, *104*, 2929.
(25) Yates, B. F.; Bouma, W. J.; Radom, L. *J. Am. Chem. Soc.* **1987**, *109*, 2250.
(26) Nobes, R. H.; Radom, L. *Chem. Phys.* **1981**, *60*, 1.
(27) Frisch, M. J.; Raghavachari, K.; Pople, J. A.; Bouma, W. J.; Radom, L. *Chem. Phys.* **1983**, *75*, 323.
(28) (a) Bouma, W. J.; MacLeod, J. K.; Radom, L. *Int. J. Mass Spectrom. Ion Phys.* **1980**, *87*, 33. (b) Bouma, W. J.; Nobes, R. H.; Radom, L. *Org. Mass Spectrom.* **1982**, *17*, 315.
(29) Osamura, Y.; Goddard, J. D.; Schaefer, H. F.; Kim, K. S. *J. Chem. Phys.* **1981**, *74*, 617.
(30) Garcia de la Vega, J. M.; Tafalla, D.; Fernandez-Alonso, J. I. *J. Mol. Struct., THEOCHEM* **1984**, *107*, 133.
(31) Frenking, G.; Heinrich, N.; Koch, W.; Schwarz, H. *Chem. Phys. Lett.* **1984**, *105*, 490.
(32) (a) Pople, J. A.; Head-Gordon, M.; Fox, D. J.; Raghavachari, K.; Curtiss, L. A. *J. Chem. Phys.* **1989**, *90*, 5622. (b) Curtiss, L. A.; Jones, C.; Trucks, G. W.; Raghavachari, K.; Pople, J. A. *J. Chem. Phys.* **1990**, *93*, 2537.
(33) Curtiss, L. A.; Raghavachari, K.; Trucks, G. W.; Pople, J. A. *J. Chem. Phys.* **1991**, *94*, 7221.
(34) (a) Curtiss, L. A.; Pople, J. A. *J. Chem. Phys.* **1988**, *88*, 7405. (b) Curtiss, L. A.; Pople, J. A. *J. Chem. Phys.* **1989**, *90*, 4314. (c) Curtiss, L. A.; Pople, J. A. *J. Chem. Phys.* **1989**, *91*, 5118. (d) Raghavachari, K.; Trucks, G. W.; Pople, J. A.; Replogle, E. *Chem. Phys. Lett.* **1989**, *158*, 207.
(35) Hehre, W. J.; Radom, L.; Schleyer, P. v. R.; Pople, J. A. *Ab Initio Molecular Orbital Theory*; Wiley: New York, 1986.
(36) Frisch, M. J.; Binkley, J. S.; Schlegel, H. B.; Raghavachari, K.; Melius, C. F.; Martin, R. L.; Stewart, J. J. P.; Bobrowicz, F. W.; Rohlfing, C. M.; Kahn, L. R.; DeFrees, D. J.; Seeger, R.; Whiteside, R. A.; Fox, D. J.; Fleuder, E. M.; Pople, J. A. GAUSSIAN 86; Carnegie-Mellon Quantum Chemistry Publishing Unit: Pittsburgh, PA, 1984.

0002-7863/91/1513-7903$02.50/0

Table I. Calculated Total Energies (hartrees) and Energy Corrections (mhartrees) Leading to G1 Total Energies (E_0, H_{298})[a]

species	MP4/6-311G(d,p)	$\langle S^2 \rangle$	$\Delta E(+)$	ΔE(2df)	ΔE(QCI)	ΔE(HLC)	ΔE(ZPE)[b]	E_0(G1)	$H_{298} - H_0$	H_{298}(G1)
1 (CH_3OH)	−115.468 47	0.000	−8.86	−59.40	−0.29	−42.98	49.41	−115.530 59	4.29	−115.526 30
2 ($CH_3OH^{\bullet+}$)	−115.076 09	0.763	−1.92	−53.32	−5.37	−37.03	46.30	−115.127 43	4.85	−115.122 58
3 ($CH_2OH_2^{\bullet+}$)	−115.093 51	0.759	−2.63	−52.52	−1.36	−37.03	47.29	−115.139 76	4.67	−115.135 09
4 ($H\cdots CH_2OH^{\bullet+}$)	−115.050 08	0.750	−2.13	−54.67	−0.28	−37.03	39.73	−115.104 46	6.16	−115.098 30
5 ($CH_3OH\cdots H^{\bullet+}$)	−115.051 58	0.750	−2.44	−54.68	−0.27	−37.03	39.98	−115.106 02	5.94	−115.100 08
6 ($CH_2O\cdots H_2^{\bullet+}$)	−115.037 61	0.787	−1.96	−52.00	−7.24	−37.03	35.29	−115.100 55	7.46	−115.093 09
7 ($CH_2O\cdots H_2^{\bullet+}$)	−115.036 92	0.786	−1.92	−51.87	−7.08	−37.03	35.14	−115.099 68	7.55	−115.092 13
8 ($HCOH\cdots H_2^{\bullet+}$)	−115.032 64	0.760	−2.10	−52.44	−1.34	−37.03	35.82	−115.089 73	7.51	−115.082 22
9 (CH_2OH^+)	−114.549 65	0.000	−1.99	−54.55	−0.29	−36.84	39.12	−114.604 20	3.89	−114.600 31
10 ($HCO\cdots H_2^+$)	−114.508 88	0.000	−1.55	−50.70	5.77	−36.84	26.27	−114.565 93	6.99	−114.558 94
11 ($COH\cdots H_2^+$)	−114.442 94	0.000	−1.48	−50.99	1.00	−36.84	23.79	−114.507 46	7.58	−114.499 88
12 (CH_2O)	−114.262 63	0.000	−6.63	−58.86	1.60	−36.84	26.07	−114.337 29	3.81	−114.333 48
13 ($CH_2O^{\bullet+}$)	−113.867 07	0.788	−1.79	−51.70	−6.58	−30.89	24.62	−113.933 41	3.86	−113.929 55
14 ($HCOH^{\bullet+}$)	−113.862 98	0.760	−1.90	−52.20	−0.77	−30.89	25.21	−113.923 53	3.89	−113.919 64
15 ($HCOH^{\bullet+}$)	−113.856 06	0.763	−1.89	−52.88	−1.02	−30.89	24.97	−113.917 77	3.90	−113.913 87
16 ($HCO\cdots H^{\bullet+}$)	−113.839 60	0.750	−1.56	−50.60	6.35	−30.89	16.54	−113.899 76	5.43	−113.894 33
17 ($COH\cdots H^{\bullet+}$)	−113.770 19	0.750	−1.56	−50.98	1.34	−30.89	12.68	−113.839 60	6.81	−113.832 79
18 ($HCO^{\bullet}$)	−113.618 95	0.766	−5.75	−57.08	2.37	−30.89	12.84	−113.697 46	3.80	−113.693 66
19 (HCO^+)	−113.339 30	0.000	−1.44	−50.44	6.35	−30.70	16.15	−113.399 38	3.42	−113.395 96
20 (COH^+)	−113.270 19	0.000	−1.43	−50.91	1.34	−30.70	12.38	−113.339 51	4.74	−113.334 77
21 (CO)	−113.098 62	0.000	−3.72	−54.20	5.06	−30.70	4.96	−113.177 22	3.30	−113.173 92
22 ($CO^{\bullet+}$)	−112.581 61	0.948	−1.76	−47.94	−9.04	−24.75	4.87	−112.660 23	3.31	−112.656 92
23 (TS, **2** → **3**)	−115.034 28	0.781	−2.61	−55.09	−1.50	−37.03	43.23	−115.087 28	4.05	−115.083 23
24 (TS, **2** → **4**)	−115.048 83	0.773	−2.56	−56.34	−1.34	−37.03	41.46	−115.104 64	4.21	−115.100 43
25 (TS, **2** → **7**)	−114.972 62	0.761	−2.52	−54.84	−2.70	−37.03	41.56	−115.028 15	4.01	−115.024 14
26 (TS, **2** → **8**)	−115.020 32	0.766	−2.94	−56.13	−1.63	−37.03	40.26	−115.077 79	4.26	−115.073 53
27 (TS, **3** → **5**)	−115.016 11	0.891	−2.72	−55.03	−7.06	−37.03	40.66	−115.077 29	4.23	−115.073 06
28 (TS, **5** → **6**)	−115.021 65	0.804	−2.28	−53.61	−6.07	−37.03	35.42	−115.085 22	4.49	−115.080 73
29 (TS, **9** → **10**)	−114.411 61	0.000	−2.44	−56.21	3.60	−36.84	30.06	−114.473 44	4.10	−114.469 34
30 (TS, **9** → **11**)	−114.372 96	0.000	−2.05	−56.15	−1.55	−36.84	30.34	−114.439 21	3.96	−114.435 25
31 (TS, **13** → **14**)	−113.797 61	0.791	−2.08	−53.05	−1.15	−30.89	18.98	−113.865 80	3.94	−113.861 86
32 (TS, **13** → **16**)	−113.829 66	0.856	−1.94	−53.68	−3.54	−30.89	16.88	−113.902 83	4.06	−113.898 77
33 (TS, **14** → **15**)	−113.833 95	0.758	−2.36	−53.99	−0.57	−30.89	21.45	−113.900 31	4.29	−113.896 02
34 (TS, **14** → **17**)	−113.766 73	0.828	−1.76	−52.91	−2.08	−30.89	13.88	−113.840 49	4.91	113.835 58
35 (TS, **15** → **16**)	−113.794 88	0.899	−1.96	−53.59	−6.90	−30.89	16.14	−113.872 08	4.06	−113.868 02
36 (TS, **15** → **17**)	−113.767 51	0.826	−1.59	−52.89	−2.00	−30.89	13.96	−113.840 92	4.89	−113.836 03
37 (H_2)	−1.167 72	0.000	0.00	0.00	−0.60	−6.14	9.45	−1.165 01	3.30	−1.161 71
38 ($H^{\bullet}$)	−0.499 81	0.750	0.00	0.00	0.00	−0.19	0.00	−0.500 00	2.36	−0.497 64

[a] The notation used is as follows: $\Delta E(+) = E$[MP4/6-311+G(d,p)] − E[MP4/6-311G(d,p)]; ΔE(2df) = E[MP4/6-311G(2df,p)] − E[MP4/6-311G(d,p)]; ΔE(QCI) = E[QCISD(T)/6-311G(d,p)] − E[MP4/6-311G(d,p)]; ΔE(HLC) = −0.19 × number of α valence electrons −5.95 × number of β valence electrons. ΔE(ZPE) = (scaled) zero-point vibrational energy correction; E(G1) = E[MP4/6-311G(d,p)] + $\Delta E(+)$ + ΔE(2df) + ΔE(QCI) + ΔE(ZPE) + ΔE(HLC). For details of G1 theory, see ref 32. [b] Calculated values of ΔE(ZPE) (mhartrees) for isotopically substituted species are as follows: **1**-d_3 40.16; **2**-d_3 37.13; **9**-d_2 33.18; **26**-d_3 33.42; **27**-d_3 33.97; **29**-d_2 24.78; **31**-d_1 16.46; **35**-d_1 13.63; **37**-d_2 6.69.

SIAN 88,[37] and GAUSSIAN 90[38] systems of programs. G1 theory is a composite procedure in which geometries are optimized at the MP2/6-31G(d) level and relative energies obtained (effectively) through quadratic configuration interaction calculations[39] with single, double, and triple excitations (QCISD(T)) with the 6-311+G(2df,p) basis set, together with isogyric and zero-point vibrational energy corrections. G2 theory is a refinement of G1 theory. It eliminates an additivity approximation used in G1 theory and employs a larger ultimate basis set, leading to results (effectively) at the QCISD(T)/6-311+G(3df,2p) level, again with isogyric and zero-point vibrational corrections. We note that neither G1 nor G2 theory is suitable for describing transition structures on reaction pathways involving a change in the number of electron pairs. None of the transition structures in the present study belong to this category. Temperature corrections to relative energies are obtained by using the calculated vibrational frequencies, scaled by 0.8929 to take into account their overestimation at the HF/6-31G(d) level. The calculated vibrational frequencies are also used to derive corrections, obtained as differences in appropriate zero-point vibrational energies, for the effect of isotopic substitution on the experimental appearance energies.

Optimized geometries are displayed in Figure 1 while calculated total energies and energy corrections are presented in Tables I and II. Calculated relative energies are compared with experimental values in Tables III–VI. Schematic energy profiles calculated at the G2 level at 0 K for the various rearrangement and fragmentation processes are shown in Figures 2–4. Because most of the experimental ionization energies and appearance energies are reported in electron volts, we have used such units in the comparison of theoretical and experimental data in Tables III–VI while standard SI units of kJ mol^{-1} are used to describe the relative energies of Figures 2–4. Relevant conversion factors are 1 hartree = 2625.5 kJ mol^{-1}, 1 eV = 96.485 kJ mol^{-1}. Unless otherwise noted, the energy comparisons in the text refer to experimental values at 298 K derived from data in the recent compendium of Lias et al.[2] The relevant heats of formation are summarized in Table VII.

We introduce the notation TS* in this paper to describe the structure on a multistep pathway from reactants to products (i.e., involving intermediate minima and transition structures) whose relative energy corresponds to the minimum energy required for that process. In the case of mass spectrometric fragmentations, such energies may be compared with appropriate experimental appearance energies. For a *direct* (one-step) transformation from reactants to products, TS* corresponds to the conventional transition structure (TS) of lowest energy for that process.

Discussion

1. Comparison of Theory with Experiment: General Remarks. Calculated relative energies are compared with available experimental values in Tables III (for species derivable from methanol), IV (for species derivable from formaldehyde), V (for species derivable from formyl radical), and VI (for species derivable from carbon monoxide). The theoretical energies used in the comparisons are generally ΔH_{298} values since these are the relative

(37) Frisch, M. J.; Head-Gordon, M.; Schlegel, H. B.; Raghavachari, K.; Binkley, J. S.; Gonzalez, C.; DeFrees, D. J.; Fox, D. J.; Whiteside, R. A.; Seeger, R.; Melius, C. F.; Baker, J.; Kahn, L. R.; Stewart, J. J. P.; Fleuder, E. M.; Topiol, S.; Pople, J. A. GAUSSIAN 88; Gaussian Inc.; Pittsburgh, PA, 1988.

(38) Frisch, M. J.; Head-Gordon, M.; Trucks, G. W.; Foresman, J. B.; Schlegel, H. B.; Raghavachari, K.; Robb, M. A.; Binkley, J. S.; Gonzalez, C.; DeFrees, D. J.; Fox, D. J.; Whiteside, R. A.; Seeger, R.; Melius, C. F.; Baker, J.; Martin, R. L.; Kahn, L. R.; Stewart, J. J. P.; Topiol, S.; Pople, J. A. GAUSSIAN 90; Gaussian Inc.; Pittsburgh, PA, 1990.

(39) Pople, J. A.; Head-Gordon, M.; Raghavachari, K. *J. Chem. Phys.* **1987**, *87*, 5968.

Table II. Calculated Total Energies (hartrees) and Energy Corrections (mhartrees) Leading to G2 Total Energies (E_0, H_{298})[a]

species	MP2/6-311G(d,p)	ΔE(+)(3df,2p)	ΔE(+)	ΔE(2df)	$\Delta\Delta E$(HLC)	E_0(G2)	H_{298}(G2)
1 (CH_3OH)	−115.436 19	−77.45	−8.66	−56.52	7.98	−115.534 88	−115.530 59
2 ($CH_3OH^{\bullet+}$)	−115.037 83	−63.44	−1.65	−50.17	6.84	−115.132 21	−115.127 36
3 ($CH_2OH_2^{\bullet+}$)	−115.062 23	−63.73	−2.41	−49.87	6.84	−115.144 37	−115.139 70
4 ($H\cdots CH_2OH^{\bullet+}$)	−115.020 16	−65.41	−1.96	−52.38	6.84	−115.108 69	−115.102 53
5 ($CH_2OH\cdots H^{\bullet+}$)	−115.021 61	−65.69	−2.26	−52.41	6.84	−115.110 20	−115.104 26
6 ($CH_2O\cdots H_2^{\bullet+}$)	−114.995 60	−62.21	−1.74	−49.21	6.84	−115.104 97	−115.097 51
7 ($CH_2O\cdots H_2^{\bullet+}$)	−114.994 99	−62.57	−1.70	−49.11	6.84	−115.104 60	−115.097 05
8 ($HCOH\cdots H_2^{\bullet+}$)	−114.997 99	−64.16	−1.91	−50.27	6.84	−115.094 87	−115.087 36
9 (CH_2OH^+)	−114.519 76	−64.49	−1.82	−52.27	6.84	−114.607 76	−114.603 87
10 ($HCO\cdots H_2^+$)	−114.478 52	−60.88	−1.40	−48.84	6.84	−114.569 73	−114.562 74
11 ($COH\cdots H_2^+$)	−114.406 20	−62.16	−1.33	−49.81	6.84	−114.511 64	−114.504 06
12 (CH_2O)	−114.235 04	−71.12	−6.48	−56.16	6.84	−114.338 93	−114.335 12
13 ($CH_2O^{\bullet+}$)	−113.832 59	−59.07	−1.58	−48.94	5.70	−113.936 26	−113.932 40
14 ($HCOH^{\bullet+}$)	−113.835 80	−60.71	−1.73	−50.04	5.70	−113.926 77	−113.922 88
15 ($HCOH^{\bullet+}$)	−113.829 21	−61.38	−1.74	−50.70	5.70	−113.921 01	−113.917 11
16 ($HCO\cdots H^{\bullet+}$)	−113.816 68	−58.29	−1.43	−48.74	5.70	−113.902 18	−113.896 75
17 ($COH\cdots H^{\bullet+}$)	−113.741 05	−59.66	−1.41	−49.79	5.70	−113.842 36	−113.835 55
18 ($HCO^{\bullet}$)	−113.593 57	−67.04	−5.51	−54.47	5.70	−113.698 82	−113.695 02
19 (HCO^+)	−113.316 40	−57.34	−1.32	−48.60	5.70	−113.401 10	−113.397 68
20 (COH^+)	−113.241 07	−59.07	−1.29	−49.72	5.70	−113.341 87	−113.337 13
21 (CO)	−113.074 48	−61.81	−3.47	−52.37	5.70	−113.177 49	−113.174 19
22 ($CO^{\bullet+}$)	−112.560 49	−54.34	−1.55	−45.91	4.56	−112.662 55	−112.659 24
23 (TS, **2** → **3**)	−115.001 04	−66.51	−2.38	−52.52	6.84	−115.092 05	−115.088 00
24 (TS, **2** → **4**)	−115.018 33	−66.85	−2.33	−53.69	6.84	−115.108 63	−115.104 42
25 (TS, **2** → **7**)	−114.934 12	−65.16	−2.24	−51.81	6.84	−115.032 42	−115.028 41
26 (TS, **2** → **8**)	−114.986 24	−67.38	−2.74	−53.57	6.84	−115.082 02	−115.077 76
27 (TS, **3** → **5**)	−114.982 80	−65.53	−2.43	−52.32	6.84	−115.081 23	−115.077 00
28 (TS, **5** → **6**)	−114.980 62	−63.60	−2.01	−50.79	6.84	−115.089 18	−115.084 69
29 (TS, **9** → **10**)	−114.382 23	−66.53	−2.22	−54.03	6.84	−114.476 88	−114.472 78
30 (TS, **9** → **11**)	−114.337 24	−66.90	−1.89	−54.41	6.84	−114.442 97	−114.439 01
31 (TS, **13** → **14**)	−113.767 18	−61.48	−1.86	−50.81	5.70	−113.868 91	−113.864 97
32 (TS, **13** → **16**)	−113.801 54	−60.64	−1.73	−51.17	5.70	−113.904 87	−113.900 81
33 (TS, **14** → **15**)	−113.807 17	−62.96	−2.29	−51.75	5.70	−113.903 53	−113.899 24
34 (TS, **14** → **17**)	−113.737 19	−60.93	−1.59	−51.26	5.70	−113.842 87	−113.837 96
35 (TS, **15** → **16**)	−113.765 26	−60.85	−1.73	−51.27	5.70	−113.874 23	−113.870 17
36 (TS, **15** → **17**)	−113.737 93	−60.95	−1.41	−51.24	5.70	−113.843 52	−113.838 63
37 (H_2)	−1.160 27	−2.49	0.00	0.00	1.14	−1.166 36	−1.163 06
38 ($H^{\bullet}$)	−0.499 81	0.00	0.00	0.00	0.00	−0.500 00	−0.497 64

[a] The notation used is as follows: ΔE(+)(3df,2p) = E[MP2/6-311+G(3df,2p)] − E[MP2/6-311G(d,p)]; ΔE(+) = E[MP2/6-311+G(d,p)] − E[MP2/6-311G(d,p)]; ΔE(2df) = E[MP2/6-311G(2df,p)] − E[MP2/6-311G(d,p)]; $\Delta\Delta E$(HLC) = 1.14 × number of valence electron pairs. E(G2) = E(G1) + ΔE(+)(3df,2p) − ΔE(+) − ΔE(2df) + $\Delta\Delta E$(HLC). For details of G2 theory, see ref 33.

Table III. Comparison of Calculated and Experimental Relative Energies for Species Derivable from Methanol (CH_3OH (**1**)) (eV)

	theory				experiment[a]	
	ΔE_0		ΔH_{298}			
species	G1	G2	G1	G2	ref 2	other
A (CH_3OH (**1**))	0	0	0	0	0	0
B (CO (**21**) + $2H_2$)	0.64	0.67	0.79	0.82	0.91	
C (CH_2O (**12**) + H_2)	0.77	0.81	0.85	0.88	0.96	
D ($HCO^{\bullet}$ (**18**) + H_2 + $H^{\bullet}$)	4.57	4.62	4.72	4.76	4.81	
E ($CH_3OH^{\bullet+}$ (**2**) + e)	10.97	10.96	10.99	10.97	10.85	10.84 [10.84] (0.01),[b] 10.84 (0.02),[c] 10.85,[d] 10.83 (0.03)[e]
F ($CH_2OH_2^{\bullet+}$ (**3**) + e)	10.64	10.63	10.65	10.64	10.54	
G (CH_2OH^+ (**9**) + $H^{\bullet}$ + e)	11.60	11.62	11.66	11.68	11.63	
H (TS*, ***E*** → ***G*** (***G***))	11.60	11.62	11.66	11.68		11.55 (0.03),[e] 11.67 (0.03),[c] 11.5 (0.1),[d] 11.58 [11.67] (0.2),[b] 11.21 [11.30] (0.3),[b] 11.67,[d] 11.6,[f] 11.58[g]
I ($CH_2O^{\bullet+}$ (**13**) + H_2 + e)	11.76	11.76	11.84	11.84	11.84	
J (TS*, ***E*** → ***I*** (**27**))	12.34	12.34	12.33	12.34		12.05 (0.12),[e] 12.21 [12.28] (0.4),[b] 12.45,[c] 16.12 [16.19] (0.5)[b]
K ($HCOH^{\bullet+}$ (**14**) + H_2 + e)	12.03	12.02	12.11	12.10	12.06	12.12[h]
L (TS, ***E*** → ***K*** (**26**))	12.32	12.32	12.32	12.32		12.34 [12.40] (0.05),[i] 12.72 [12.78] (0.3)[b]
M (HCO^+ (**19**) + H_2 + $H^{\bullet}$ + e)	12.69	12.72	12.82	12.85	12.91	
N (TS*, ***E*** → ***M*** (***M***))	12.69	12.72	12.82	12.85		12.88 [13.05] (0.1),[i] 13.06 (0.1),[e] 14.0 (0.2),[d] 14.82 (0.2),[j] 14.38 (0.5),[b] 14.0[f]
O (TS*, ***K*** → ***M*** (**35**))	13.43	13.45	13.51	13.53		13.8 [13.9] (0.2),[i] 14.0 (0.2),[k] 13.43 [13.53] (0.5)[b]
P (TS*, ***K*** → ***I*** → ***M*** (**31**))	13.60	13.60	13.68	13.68		13.8 [13.9] (0.2),[i] 13.7 [13.8] (0.6)[b]
Q (TS, ***G*** → ***M*** (**29**))	15.16	15.18	15.22	15.24		15.1 (0.1),[i] 14.7 (0.3),[d] 14.66 [14.77] (0.5)[b]
R (COH^+ (**20**) + H_2 + $H^{\bullet}$ + e)	14.32	14.33	14.48	14.50	14.33	14.61[m]
S (TS*, ***E*** → ***R*** (***R***))	14.32	14.33	14.48	14.50		16.25 (0.27)[j]
T ($CO^{\bullet+}$ (**22**) + $2H_2$ + e)	14.70	14.68	14.86	14.84	14.92	
U (HCO^+ (**19**) + $3H^{\bullet}$ + e)	17.18	17.25	17.35	17.42	17.42	

[a] In those cases where the experimental appearance energies refer to ions derived from CD_3OH rather than CH_3OH, corrections for isotope effects, derived from the calculated zero-point vibrational energies (footnote *b* of Table I), are applied. The uncorrected values in these cases are shown in square brackets. [b] From ref 3. [c] From ref 4. [d] From ref 5. [e] From ref 6. [f] From ref 7. [g] From ref 8. [h] From ref 9. [i] From ref 10 [j] From ref 11. [k] From ref 12. [l] From ref 13. [m] From ref 14.

Table IV. Comparison of Calculated and Experimental Relative Energies for Species Derivable from Formaldehyde (CH_2O (**12**)) (eV)

	theory				experiment	
	ΔE_0		ΔH_{298}			
species	G1	G2	G1	G2	ref 2	other
V (CH_2O (**12**))	0	0	0	0	0	0
W ($CH_2O^{\bullet+}$ (**13**) + e)	10.99	10.96	10.99	10.96	10.88	10.87 (0.005),[a] 10.88 (0.02),[b] 10.88 (0.04),[c] 10.83 (0.1),[d] 10.86[e]
X ($HCOH^{\bullet+}$ (**14**) + e)	11.26	11.22	11.26	11.22	11.10	11.16[f]
Y (HCO^+ (**19**) + $H^\bullet$ + e)	11.92	11.91	11.97	11.97	11.94	
Z (TS, ***W*** → ***Y*** (***Y***))	11.92	11.91	11.97	11.97		11.93 (0.01),[a] 11.95 (0.06),[b] 11.89 (0.03),[g] 12.46 (0.2),[d] 11.97[e]
A' (COH^+ (**20**) + $H^\bullet$ + e)	13.55	13.53	13.63	13.62	13.37	13.64[h]
B' ($CO^{\bullet+}$ (**22**) + H_2 + e)	13.93	13.88	14.01	13.95	13.96	
C' (TS, ***W*** → ***B'*** (***B'***))	13.93	13.88	14.01	13.95		14.10 (0.08)[a]

[a] From ref 15. [b] From ref 16. [c] From ref 17. [d] From ref 18. [e] From ref 8. [f] From ref 9. [g] From ref 6. [h] From ref 14.

Table V. Comparison of Calculated and Experimental Relative Energies for Species Derivable from Formyl Radical ($HCO^\bullet$ (**18**)) (eV)

	theory				experiment	
	ΔE_0		ΔH_{298}			
species	G1	G2	G1	G2	ref 2	other
D' ($HCO^\bullet$ (**18**))	0	0	0	0	0	0
E' (HCO^+ (**19**) + e)	8.11	8.10	8.10	8.09	8.10	8.27 (0.01),[a] 8.10 (0.05),[b] 8.13 (0.13)[c]
F' (COH^+ (**20**) + e)	9.74	9.71	9.77	9.74	9.52	9.80[d]
G' ($CO^{\bullet+}$ (**22**) + $H^\bullet$ + e)	14.62	14.59	14.67	14.64	14.63	

[a] From ref 19. [b] From ref 8. [c] From ref 6. [d] From ref 14.

Table VI. Comparison of Calculated and Experimental Relative Energies for Species Derivable from Carbon Monoxide (CO (**21**)) (eV)

	theory				experiment	
	ΔE_0		ΔH_{298}			
species	G1	G2	G1	G2	ref 2	other
H' (CO (**21**))	0	0	0	0	0	0
I' ($CO^{\bullet+}$ (**22**) + e)	14.07	14.01	14.07	14.01	14.01	

Table VII. Experimental Heats of Formation (kJ mol^{-1})[a]

species	$\Delta H_f°_{298}$	species	$\Delta H_f°_{298}$
CH_3OH	−201.6	$HCO^\bullet$	44.8
$CH_3OH^{\bullet+}$	845.3	HCO^+	825.6
$CH_2OH_2^{\bullet+}$	815	COH^+	963
CH_2OH^+	703	CO	−113.80
CH_2O	−108.7	$CO^{\bullet+}$	1238.32
$CH_2O^{\bullet+}$	940.5	$H^\bullet$	217.999
$HCOH^{\bullet+}$	962		

[a] From ref 2.

energies most commonly available experimentally. However, for comparisons with spectroscopic determinations of ionization energies, ΔE_0 values are more appropriate, while for appearance energies determined from photoionization experiments, the threshold energy has been argued[40] to correspond to ions with 0 K internal energy and the translational energy of the precursor molecules, so that a correction to the ΔH_{298} values would be appropriate. The latter corrections are typically quite small (0.04 eV) and, because we are dealing with a variety of experimental techniques in the present study, are not incorporated here. They would, however, have the effect of slightly lowering the calculated appearance energies. Experimental energies for stable species are derived, where possible, from $\Delta H_f°_{298}$ values in the compendium of Lias et al. (LBLHLM),[2] as listed in Table VII. Appearance energy and some additional ionization energy values have been taken from the original literature. In those cases where the experimental appearance energies refer to ions derived from CD_3OH rather than CH_3OH, corrections for isotope effects, derived from the calculated zero-point vibrational energies for the appropriate isotopically substituted species, are applied.

We examine initially the relative energies in Tables III–VI for which relevant data are available in LBLHLM[2] (21 comparisons). It is pleasing to see that there is good agreement between theory and experiment, the larger differences occurring only for comparisons involving either $HCOH^{\bullet+}$ or COH^+. In the case of $HCOH^{\bullet+}$, we have recently questioned[9] the experimental value of the heat of formation that had been derived assuming a zero reverse activation barrier for the fragmentation process from methanol. Use of our new suggested $\Delta H_f°_{298}$ value for $HCOH^{\bullet+}$ of 968 kJ mol^{-1}, obtained by combining the experimental appearance energy with the calculated reverse activation energy, leads to good agreement between theory and experiment for the relevant comparisons in Tables III and IV. For COH^+, we note that the experimental $\Delta H_f°_{298}$ listed in LBLHLM[2] (963 kJ mol^{-1}) is based on a correlation between proton affinities of oxygen bases and O_{1S} binding energies from ESCA experiments[20] rather than from a direct experimental determination. An alternative but again indirect experimental estimate of $\Delta H_f°_{298}$ for COH^+ (990 kJ mol^{-1}) has been obtained[14] from an empirical relationship between proton affinities and rates of proton-transfer reactions. Our present results suggest a value of 983 kJ mol^{-1} for $\Delta H_f°_{298}$ for COH^+.

If we exclude those comparisons within Tables III–VI involving COH^+ and $HCOH^{\bullet+}$, for which we have just noted reasons why the standard experimental $\Delta H_f°_{298}$ values might be questioned, the remaining 16 relative energies show a mean absolute difference between theory and experiment of 0.07 eV (G1) or 0.05 eV (G2). The G2 results are almost always slightly closer to the experimental values. The discrepancy between G2 and experiment exceeds the 0.1-eV target in only one case (the ionization energy of methanol), while at the G1 level there are four such cases. We note that the good agreement between theory and experiment comes despite substantial spin contamination in some cases, e.g., $\langle S^2 \rangle$ = 0.948 for $CO^{\bullet+}$ (Table I). In these cases, the ΔE(QCI) correction is found to be significant (e.g., 0.38 eV for the ionization energy of CO). Our present results provide further support for the usefulness of the quadratic configuration interaction procedure in satisfactorily handling such situations.[32]

The remaining relative energies in Tables III–VI (10 comparisons) refer to appearance energies and potentially provide a measure of the performance of G1 and G2 theories in estimating the energies of transition structures for chemical reactions. The differences between G1 and G2 relative energies for the transition structures are uniformly small and significantly smaller than the uncertainties in the experimental results. Unfortunately, the separate experimental determinations of appearance energies often span a wide range of values, reflecting the inherent difficulties in determining the energy threshold in such experiments. The theoretical values generally lie within the experimental range and within 0.15 eV of what are assessed as the most accurate ex-

(40) Traeger, J. C.; McLoughlin, R. G. *J. Am. Chem. Soc.* **1981**, *103*, 3647.

perimental values. In only one case is the discrepancy between theory and experiment significantly greater than 0.15 eV, and we believe, as discussed below, that there are grounds for questioning the experimental result in this instance.

Having noted, consistent with previous findings,[33] that the G2 relative energies are generally in slightly better agreement with experiment than are the G1 values, we restrict the comparisons in the remainder of the paper to the G2 results.

2. Species Derivable From Methanol (1). We begin our discussion by examining the energies of individual species which can be produced from processes that start with neutral methanol (Table III). Energies quoted in this section, unless otherwise noted, are values relative to neutral methanol.

Carbon Monoxide (21) + $2H_2$ (*B*). The energies required for this comparison are all well established experimentally. The difference between the calculated value for ***B*** of 0.82 eV and the experimental value of 0.91 eV lies within the target range of 0.1 eV.

Formaldehyde (12) + H_2 (*C*). The difference between the calculated value for ***C*** of 0.88 eV and the experimental value of 0.96 eV again lies within the target of 0.1 eV.

Formyl Radical (18) + H_2 + H$^\bullet$ (*D*). There is good agreement between the calculated (4.76 eV) and experimental (4.81 eV) energies for ***D***, supporting the choice of $\Delta H_f°_{298}$ for HCO$^\bullet$ in the LBLHLM compendium.[2]

Methanol Cation (2) + e (*E*). The ionization energy of methanol is well determined experimentally. The discrepancy between the theoretical value (10.96 eV at 0 K) and the selected[2] experimental value (10.85 eV) is somewhat greater than errors found previously at the G2 level for the ionization energies of simpler systems[33] and lies just outside the 0.1-eV target. As we shall see below, the geometry of **2** changes significantly in going from the HF/3-21G to HF/6-31G(d) to MP2/6-31G(d) levels. The error in the G2 ionization energy may partly reflect a residual error in the calculated structure of **2**.

There are interesting features of the structure of $CH_3OH^{\bullet+}$ (**2**; Figure 1) that deserve comment. Whereas at simpler levels of theory (e.g., HF/3-21G) **2** has a preferred eclipsed structure of C_s symmetry,[25] the preferred structure at the HF/6-31G(d) level has C_1 symmetry.[27] The asymmetric distortion is much more pronounced in the MP2/6-31G(d) structure reported here and may be attributed to hyperconjugative interaction between one of the methyl C–H bonds and the 2p orbital at oxygen perpendicular to the COH plane (2p(O)), as displayed in **39**. The

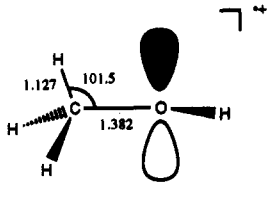

39

MP2/6-31G* geometry shows the striking consequences of such hyperconjugative interaction:[41] The C–H bond makes a dihedral angle of 103.4° with the O–H bond, resulting in an alignment almost parallel to the 2p(O) orbital, its length (1.127 Å) is increased considerably from that of normal methyl C–H bonds, the HCO bond angle has narrowed to 101.5°, and the C–O bond at 1.382 Å appears to reflect some double bond character. The structure found here for the methanol cation is analogous in some respects to the twisted structure recently reported[42] for the prop-2-yl cation, although the hyperconjugative interaction shown in **39** is not as strong.

Methyleneoxonium Radical Cation (3) + e (*F*). The methyleneoxonium radical cation ($CH_2OH_2^{\bullet+}$, **3**) has received much attention as a prototype distonic radical cation,[43,44] from both a theoretical[24,25,27] and experimental[45,46] point of view, and will not be discussed in detail here. We note simply that the calculated relative energy for ***F*** of 10.64 eV is in satisfactory agreement with the experimental value of 10.54 eV.

The present calculations represent the highest level treatment reported to date of the rearrangement of $CH_3OH^{\bullet+}$ (**2**) to $CH_2OH_2^{\bullet+}$ (**3**) (Figure 2). The calculated energy difference between **2** and **3** is 32 kJ mol^{-1} in favor of $CH_2OH_2^{\bullet+}$ (**3**), in close agreement with the experimental energy difference of 30 kJ mol^{-1} (Table VII). The effect of quadratic CI is quite large for **2** (Table I), leading to a significant change from the previous best theoretical estimate for the energy difference (46 kJ mol^{-1}).[25] The G2 value of the barrier separating **2** from **3** (via **23**) (105 kJ mol^{-1}) is, however, close to the previous value (108 kJ mol^{-1}).[25] The energy of **23** relative to neutral methanol (12.05 eV) represents our prediction of the appearance energy for $CH_2OH_2^{\bullet+}$ (**3**) produced from methanol.

Hydroxymethyl Cation (9) + H$^\bullet$ + e (*G*). The calculated relative energy for ***G*** (11.68 eV) is very close to the experimental value (11.63 eV).

At the MP2/6-31G(d) level, elimination of a hydrogen atom from $CH_3OH^{\bullet+}$ (**2**) to give CH_2OH^+ (**9**) proceeds via transition structure **24**. However, at the G2 level, **24** lies lower in energy than CH_2OH^+ (**9**) + H$^\bullet$ or the weak complex H···$CH_2OH^{\bullet+}$ (**4**) (Figure 2), suggesting that there may in fact be no reverse barrier for the hydrogen atom elimination. This result is consistent with experimental appearance energy measurements that yield values (Table III) close to the thermochemical threshold for formation of CH_2OH^+ (**9**) + H$^\bullet$. Our calculated relative energy for ***G*** (11.68 eV) is in satisfactory agreement with the best experimental values (11.5–11.67 eV).[3-8]

The reverse reaction of addition of H$^\bullet$ to CH_2OH^+ (**9**) is of interest from the point of view of the comparison of ease of addition to carbon versus oxygen. In the case of addition of H$^\bullet$ to HCO^+, Frenking et al.[31] were able to rationalize the observation[10] of more facile addition to carbon (yielding $CH_2O^{\bullet+}$) in preference to oxygen (which would give $HCOH^{\bullet+}$) by use of frontier orbital arguments: The lowest unoccupied molecular orbital (LUMO) of HCO^+ is concentrated on C rather than O, and therefore interaction of H$^\bullet$ at C is more favorable. A similar argument would apply to the addition of H$^\bullet$ to CH_2OH^+ for which it had previously been noted[24] that addition at C is again preferred over that at O. Our calculations suggest that addition at C (yielding $CH_3OH^{\bullet+}$ (**2**)) is probably barrier-free whereas addition at O (yielding the thermodynamically more stable $CH_2OH_2^{\bullet+}$ (**3**)) requires a barrier of 70 kJ mol^{-1} (Figure 2). Thus, in this case (in contrast to addition to HCO^+), the lower barrier is associated with the higher energy product.

Formaldehyde Cation (13) + H_2 + e (*I*). Our calculated relative energy for ***I*** (11.84 eV) coincides with the experimental value (11.84 eV).[2]

We find that the lowest energy pathway for production of $CH_2O^{\bullet+}$ (**13**) from methanol (**1**) proceeds via $CH_3OH^{\bullet+}$ (**2**), $CH_2OH_2^{\bullet+}$ (**3**), and the weak complex CH_2OH···$H^{\bullet+}$ (**5**) (Figure 3). The highest point on this pathway involves **27**, the transition structure between **3** and **5**, at point ***J*** of the surface. Our calculated energy for ***J*** (12.34 eV) lies within the range of the majority of the experimental values (12.05–12.45 eV)[3,4,6] reported for the appearance energy of $CH_2O^{\bullet+}$ (**13**). Interestingly, Momigny et al.[3] found a threshold appearance energy for production of $CD_2O^{\bullet+}$ (**13**) from CD_3OH (**1**) of 12.28 ± 0.4 eV, in satisfactory agreement with our calculated value. However, they interpreted this to be due to an impurity ($CDHOH^+$) of the same

(41) The structural consequences of hyperconjugation are discussed in Radom, L. *Prog. Theor. Org. Chem.* **1982**, *3*, 1.

(42) Schleyer, P. v. R.; Koch, W.; Liu, B.; Fleischer, U. *J. Chem. Soc., Chem. Commun.* **1989**, 1098.

(43) (a) Yates, B. F.; Bouma, W. J.; Radom, L. *J. Am. Chem. Soc.* **1984**, *106*, 5805. (b) Radom, L.; Bouma, W. J.; Nobes, R. H.; Yates, B. F. *Pure Appl. Chem.* **1984**, *56*, 1831.

(44) For a recent comprehensive review, see: Hammerum, S. *Mass Spectrom. Rev.* **1988**, *7*, 123.

(45) Bouma, W. J.; MacLeod, J. K.; Radom, L. *J. Am. Chem. Soc.* **1982**, *104*, 2930.

(46) Holmes, J. L.; Lossing, F. P.; Terlouw, J. K.; Burgers, P. C. *J. Am. Chem. Soc.* **1982**, *104*, 2931.

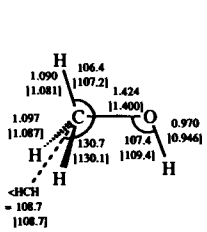

1 (C_s)

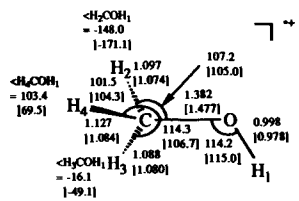

2 (C_1)

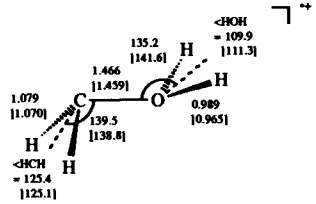

3 (C_s)

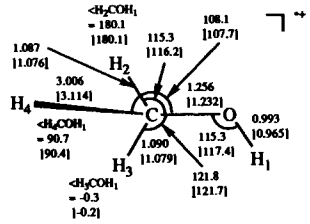

4 (C_1)

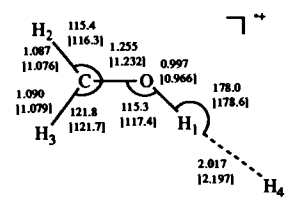

5 (C_s)

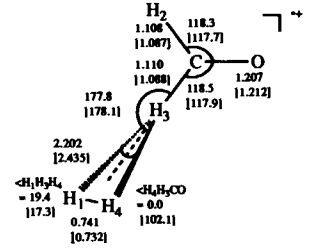

6 (C_s)

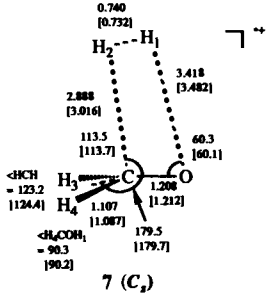

7 (C_s)

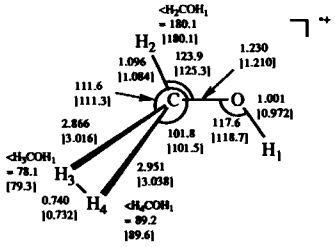

8 (C_1)

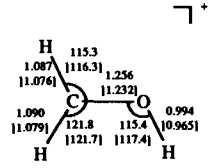

9 (C_s)

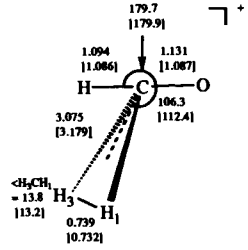

10 (C_s)

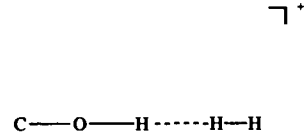

11 ($C_{\infty v}$)

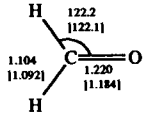

12 (C_{2v})

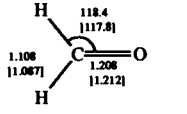

13 (C_{2v})

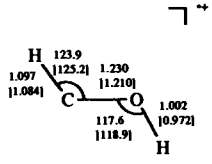

14 (C_s)

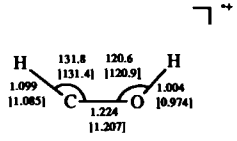

15 (C_s)

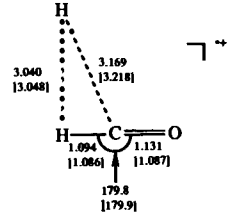

16 (C_s)

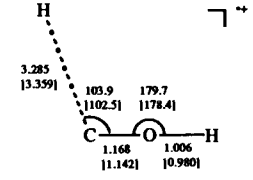

17 (C_s)

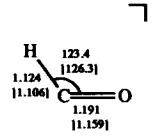

18 (C_s)

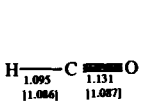

19 ($C_{\infty v}$)

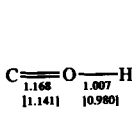

20 ($C_{\infty v}$)

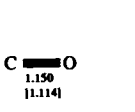

21 ($C_{\infty v}$)

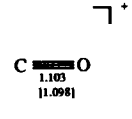

22 ($C_{\infty v}$)

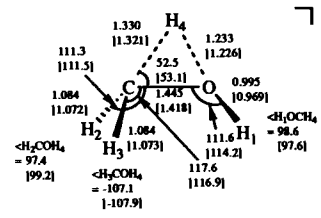

23 (C_1)

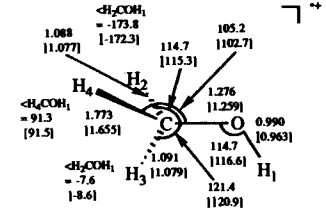

24 (C_1)

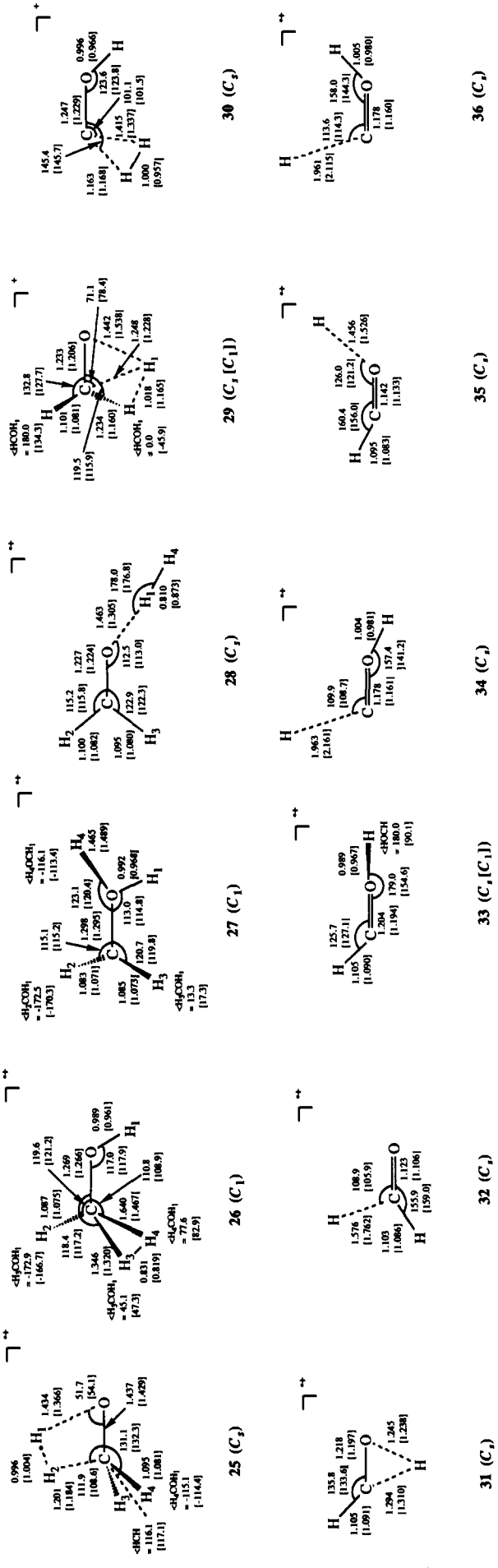

Figure 1. Optimized structures for methanol, the possible products of its dissociative ionization, and relevant transition structures (MP2/6-31G(d) values with HF/6-31G(d) values in square brackets).

nominal mass, and preferred a value of 16.19 eV for the appearance energy of $CD_2O^{\bullet+}$ (**13**). Our results would clearly support the lower value.

Hydroxymethylene Cation (14) + H_2 + e (*K*). The calculated relative energy (12.10 eV) of ***K*** is in good agreement with the experimental value (12.06 eV) derived from LBLHLM.[2] Even better agreement comes from the use of our recently revised[9] $\Delta H_f°_{298}$ value for $HCOH^{\bullet+}$ (**14**) (968 kJ mol^{-1}) that leads to a relative energy of 12.12 eV. As previously noted,[9] the revised $\Delta H_f°_{298}$ value gives an energy difference between $CH_2O^{\bullet+}$ (**13**) and $HCOH^{\bullet+}$ (**14**) of 27 kJ mol^{-1}, in close agreement with the present G2 value (25 kJ mol^{-1}).

The $HCOH^{\bullet+}$ radical cation exists as anti (**14**) and syn (**15**) isomers, the former lying lower in energy by 15 kJ mol^{-1}. The barrier separating **15** from **14** (at transition structure **33**) is 46 kJ mol^{-1}. Whereas, at the HF/6-31G(d) level, the syn–anti transformation takes place via a rotation–inversion pathway, on the MP2/6-31G(d) potential energy surface the pathway corresponds to pure in-plane inversion. This is reflected in the structures calculated for **33**, as displayed in Figure 1.

The $HCOH^{\bullet+}$ radical cation (**14**) may be formed by elimination of molecular hydrogen from $CH_3OH^{\bullet+}$ (**2**) via transition structure **26** (***L***, Figure 4). The calculated relative energy of ***L*** (12.32 eV) is in good agreement with the experimental appearance energy after correction for isotope effects (12.34 eV) of Burgers et al.[10] As pointed out previously,[9] it is essential to take into account the reverse activation energy for this process in deriving the heat of formation of $HCOH^{\bullet+}$ (**14**) from the experimental appearance energy.

Formyl Cation (19) + H_2 + $H^{\bullet}$ + e (*M*). Again, the calculated energy (12.85 eV) of ***M*** is in satisfactory agreement with the experimental value (12.91 eV).

We have characterized several different pathways by which HCO^+ (**19**) can be produced from methanol (**1**). These will be discussed in turn and the calculated energy requirements compared with appropriate experimental appearance energies.

First, and very importantly, is the prediction of a pathway in which HCO^+ (**19**) can be produced at thermochemical threshold. This proceeds via $CH_3OH^{\bullet+}$ (**2**) and $CH_2OH_2^{\bullet+}$ (**3**), the complexes $CH_2OH\cdots H^{\bullet+}$ (**5**) and $CH_2O\cdots H_2^{\bullet+}$ (**6**), and $CH_2O^{\bullet+}$ (**13**) (Figure 3). We note that the energy of the MP2/6-31G(d) transition structure (**32**) separating $H\cdots CHO^{\bullet+}$ (**16**) from $CH_2O^{\bullet+}$ (**13**) drops below that of **16** at the G2 level. Thus, we predict that there is little or no barrier for addition of $H^{\bullet}$ to the carbon of HCO^+ to produce $CH_2O^{\bullet+}$ (**13**). The experimental values of the appearance energy of HCO^+ (**19**) from methanol span a wide range, 13.05–14.82 eV (before correction for isotope effects),[3,5–7,10,11] but are all higher than the experimental thermochemical threshold (12.91 eV).[2] The lowest values are associated with the smallest quoted experimental uncertainties and are therefore taken as being the most reliable. In these studies, it was noted[10,21] "that the experimental ionization efficiency curve tailed badly, becoming asymptotic to the energy axis". Both this comment and the wide range of reported values would seem to indicate that experimental observation of the threshold appearance energy for HCO^+ (**19**) from methanol is not straightfoward. This may be associated with the complicated pathway that takes **1** to **19**. The isotope effect for this particular process also turns out to be significant. Thus, the value of 13.05 ± 0.1 eV obtained by Burgers et al.[10] for the appearance energy of HCO^+ from CD_3OH needs to be corrected by 0.17 eV to give an estimate of the experimental appearance energy for production of HCO^+ from CH_3OH. The value obtained in this manner is 12.88 eV, which is very close to our calculated value of 12.85 eV. Our results for this process emphasize that care should be taken to account for the effect of isotopic substitution in appearance energy measurements. We note that production of HCO^+ from $CD_3OH^{\bullet+}$ requires an initial reversible formation of $CD_2OHD^{\bullet+}$ (**3**).

We also note in passing that the appearance energy for HCO^+ reported by Harland et al.[11] (14.82 eV) differs from our calculated value by about 2 eV and is also considerably higher than the other experimental values. This will be relevant to our discussion of

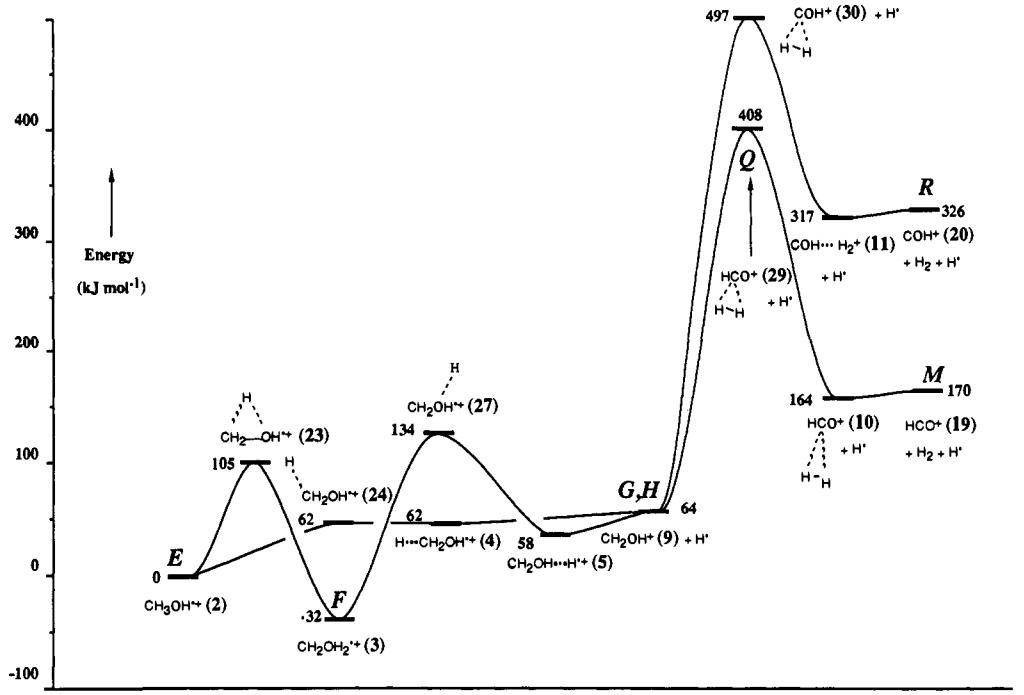

Figure 2. Schematic energy profile for rearrangement and fragmentation reactions of ionized methanol involving CH_2OH^+ (**9**) as an intermediate (G2 level at 0 K).

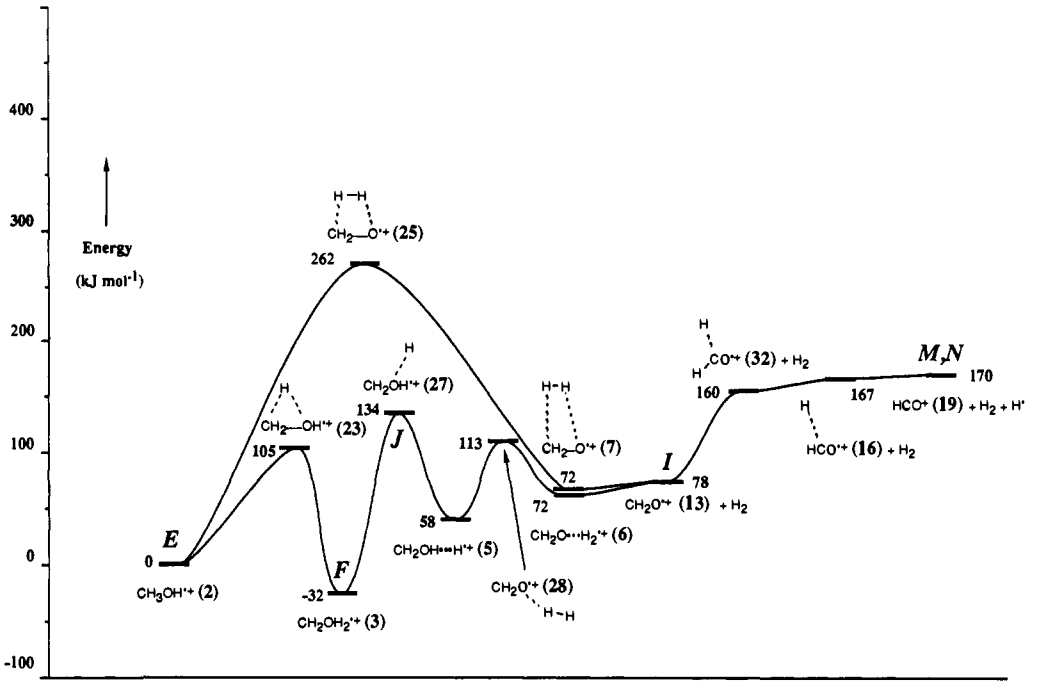

Figure 3. Schematic energy profile for rearrangement and fragmentation reactions of ionized methanol including lowest energy production of $CH_2O^{+\bullet}$ (**13**) (G2 level at 0 K).

the appearance energy of COH^+ below.

The mass spectrometry experiments not only allow the determination of the threshold appearance energy for HCO^+ (**19**) produced from CH_3OH (**1**) but also, through analysis of metastable decompositions, appearance energies for HCO^+ produced by various other higher energy mechanisms. After the threshold reaction, the process of next lowest energy requirement is production of HCO^+ from $HCOH^{+\bullet}$ (**14**). In this case, labeling experiments are able to distinguish between *direct* production of HCO^+ from $HCOH^{+\bullet}$ and *indirect* production of HCO^+ via $CH_2O^{+\bullet}$ (**13**). Thus, starting with $DCOH^{+\bullet}$ from CD_3OH, the threshold for loss of $H^\bullet$ corresponds to direct production of DCO^+ whereas loss of $D^\bullet$ corresponds to reaction via $HDCO^{+\bullet}$. The former proceeds via transition structure **35** (***O***, Figure 4) and has a calculated energy requirement of 13.53 eV. The experimental values range from 13.43 to 14.0 eV.[3,10,12]

Initially, loss of $D^\bullet$ from $DCOH^{+\bullet}$ had been assumed to correspond to formation of COH^+ (**20**),[10,13] but theoretical calculations[21] subsequently indicated that this would require considerably greater energy and that a lower energy loss of $D^\bullet$ could take place via initial hydrogen migration to $HDCO^{+\bullet}$ followed by $D^\bullet$ loss to give a fragment ion with the HCO^+ (**19**) rather than COH^+ (**20**) structure. The nature of the m/z 29 ion was confirmed in collisional activation mass spectrometry experiments.[21] Our calculated energy for ***P*** (13.68 eV) corresponds to the relative energy of the transition structure **31** separating $HCOH^{+\bullet}$ (**14**) from $CH_2O^{+\bullet}$ (**13**), and **31** is the highest point on the reaction pathway leading to HCO^+ (**19**) from $HCOH^{+\bullet}$ (**14**) via $CH_2O^{+\bullet}$

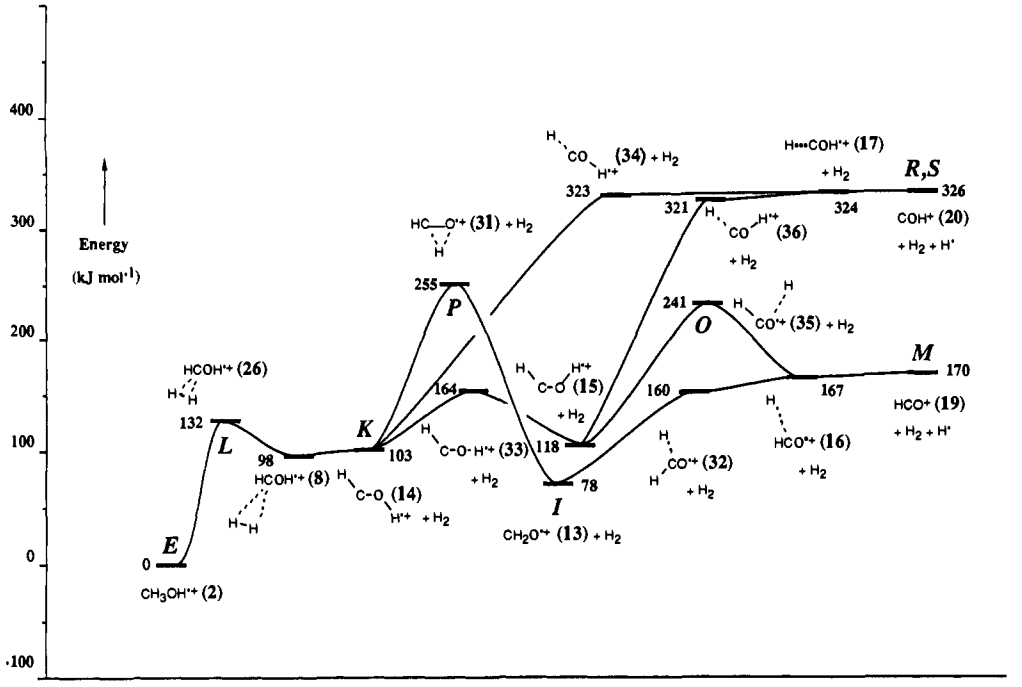

Figure 4. Schematic energy profile for rearrangement and fragmentation reactions of ionized methanol involving $HCOH^{\bullet+}$ (**14**) as an intermediate (G2 level at 0 K).

(**13**). The calculated relative energy is in satisfactory agreement with the two (corrected) experimental values (13.7, 13.8 eV) for the appearance energy of HCO^+ from CD_3OH.

Finally, HCO^+ (**19**) can be produced via CH_2OH^+ (**9**). Both theory and experiment agree that this is a high-energy process. The calculated energy (15.24 eV), corresponding to the relative energy of the transition structure **29** separating CH_2OH^+ (**9**) from HCO^+ (**19**) (*Q*, Figure 2), is in good agreement with the appearance energy (15.1 eV) reported by Wijenberg et al.[13]

The unimolecular elimination of molecular hydrogen from CH_2OH^+ (**9**) has been examined in several experimental studies[47-49] which showed (a) that HCO^+ rather than COH^+ is produced, (b) the hydroxyl hydrogen is always eliminated, and (c) that there is considerable kinetic energy released, indicating a substantial reverse activation barrier. This process was also examined theoretically by Wijenberg et al.,[13] who found an asymmetric nonplanar transition structure, the asymmetry being consistent with the results of the labeling experiments. Their calculated barrier of 372 kJ mol^{-1} was, however, somewhat higher than the experimental value of 339 kJ mol^{-1}. We also find a nonplanar structure for **29** at the HF/6-31G(d) level but find that at MP2/6-31G(d) a planar structure is preferred. Our calculated barrier for the H_2 elimination is 344 kJ mol^{-1}, very close to the experimental value.

Isoformyl Cation (20) + H_2 + H• + e (*R*). The calculated relative energy for *R* (14.50 eV) differs from the LBLHLM value (14.33 eV) by 0.17 eV. We note that use of the $\Delta H_f°_{298}$ value of 983 kJ mol^{-1} suggested in section 1 for COH^+ leads to a relative energy of 14.54 eV. The G2 estimate of the energy difference between HCO^+ and COH^+ is 156 kJ mol^{-1} in favor of HCO^+.

At the MP2/6-31G(d) level, COH^+ (**20**) may be produced from *anti*-$HCOH^{\bullet+}$ (**14**) via transition structure **34** or from *syn*-$HCOH^{\bullet+}$ (**15**) via transition structure **36** (Figure 4). However, at the G2 level, **34** and **36** both drop below the energy of COH^+ + H• and the weak complex H···$COH^{\bullet+}$ (**17**) (Figure 4), so we predict that COH^+ (**20**) should be observable close to the thermochemical threshold (14.50 eV). The only experimental value[11] that we are aware of is 16.25 eV, i.e., more than 1.7 eV higher than our predicted value. We note, however, that the same experimental study[11] reported a value for the appearance energy of HCO^+ that differed from other experimental values by nearly 2 eV. We therefore feel that our theoretical result provides the most reliable current estimate of the appearance energy for COH^+ production from methanol.

Carbon Monoxide Cation (22) + $2H_2$ + e (*T*). The calculated relative energy (14.84 eV) is in satisfactory agreement with the experimental value (14.92 eV).

Formyl Cation (19) + 3H• + e (*U*). The calculated relative energy in this case (17.42 eV) actually coincides with the experimental value (17.42 eV).

3. Species Derivable from Formaldehyde (12). Energies relative to formaldehyde (**12**) are listed in Table IV.

Formaldehyde Radical Cation (13) + e (*W*). The ionization energy of formaldehyde is experimentally well established, the selected value in the LBLHLM compendium[2] being 10.88 eV. As in the case of methanol, our calculated ionization energy (10.96 eV) is somewhat too high but lies within the 0.1-eV target.

Hydroxymethylene Radical Cation (14) + e (*X*). The energy for $HCOH^{\bullet+}$ (**14**) relative to neutral formaldehyde obtained from LBLHLM[2] is 11.10 eV, 0.12 eV lower than our calculated value of 11.22 eV. An alternative experimental estimate of 11.16 eV comes from using our revised $\Delta H_f°_{298}$ value for $HCOH^{\bullet+}$, and this brings theory and experiment into closer agreement.

Formyl Cation (19) + H• + e (*Y*). The calculated relative energy for *Y* (11.97 eV) agrees well with the experimental value (11.94 eV).[2]

There are several experimental estimates of the appearance energy of HCO^+ (**19**) produced from CH_2O (**12**). Most are clustered in the range 11.93–11.97 eV (*Z*, Table IV),[6,15,16,18] indicating that this reaction can take place at the thermochemical threshold. This is in agreement with our calculations, which indicate no reverse barrier for the decomposition process (Figure 3).

Isoformyl Cation (20) + H• + e (*A'*). The calculated relative energy of *A'* (13.62 eV) differs from the experimental value (13.37 eV) by 0.25 eV. As noted above, the origin of this discrepancy appears to be associated with a discrepancy between theoretical and experimental energies for COH^+ (**13**). Use of the $\Delta H_f°_{298}$ value of 983 kJ mol^{-1} for COH^+ leads to an energy for *A'* of 13.57 eV, only 0.05 eV from the calculated result.

Carbon Monoxide Cation (22) + H_2 + e (*B'*). The calculated relative energy of *B'* (13.95 eV) is close to the experimental value (13.96 eV).

(47) Williams, D. H.; Hvistendahl, G. *J. Am. Chem. Soc.* **1974**, 96, 6753.
(48) Richard, G. J.; Cole, N. W.; Christie, J. R.; Derrick, P. J. *J. Am. Chem. Soc.* **1978**, *100*, 2904.
(49) Hvistendahl, G.; Uggerud, E. *Org. Mass Spectrom.* **1985**, *20*, 541.

Our calculations indicate that elimination of molecular hydrogen from $CH_2O^{\bullet+}$ (**13**) can take place without a reverse barrier, corresponding to an energy relative to CH_2O (**12**) of 13.95 eV. The experimental appearance energy for $CO^{\bullet+}$ (**22**) from CH_2O is 14.10 eV (*C'*), 0.15 eV higher than our predicted value, perhaps indicating difficulty in observing threshold formation.

4. Species Derivable from Formyl Radical (18). Energies relative to formyl radical (**18**) are listed in Table V.

Formyl Cation (19) + e (*E'*). The ionization energy for $HCO^{\bullet}$ given in LBLHLM[2] is 8.10 eV, which coincides with our calculated value (8.10 eV at 0 K). Dyke et al.[19] recorded the photoelectron spectrum of $HCO^{\bullet}$ (**18**) and deduced an ionization energy of 8.27 eV. However, their analysis was complicated by the fact that they were not able to observe the lowest transitions because of poor Franck–Condon overlap, arising from the markedly different geometries of **18** (bent) and **19** (linear). Our result is in close agreement with the results of Traeger (8.10 eV)[8] and Warneck (8.13 eV).[6]

Isoformyl Cation (20) + e (*F'*). Again, the difference between calculated (9.74 eV) and experimental (9.52 eV) relative energies for *F'* reflects a discrepancy between theoretical and experimental energies for COH^+ (**13**). Again we note that a $\Delta H_f°_{298}$ value of 983 kJ mol^{-1} for COH^+ would lead to good agreement between theory and experiment in this case (9.72 eV) and thus for all three comparisons in Tables III–V involving COH^+.

Carbon Monoxide Cation (22) + H$^{\bullet}$ + e (*G'*). The calculated relative energy (14.64 eV) is very close to the experimental value (14.63 eV).

5. Species Derivable from Carbon Monoxide (21). Energies relative to carbon monoxide (**21**) are listed in Table VI.

Carbon Monoxide Cation (22) + e (*I'*). The ionization energy of carbon monoxide is well established experimentally at 14.01 eV, which coincides with our calculated value (14.01 eV).

6. Ion-Neutral Complexes. There has been continuing recent interest in the possible involvement of ion–neutral complexes in mass spectrometric fragmentation reactions.[50] Our calculations reveal several instances where such complexes play an important role for the reactions examined here. One striking example is the lowest energy pathway for production of $CH_2O^{\bullet+}$ (**13**) from $CH_2OH_2^{\bullet+}$ (**3**) (Figure 3). This involves the weak complex $CH_2OH\cdots H^{\bullet+}$ (**5**), which allows subsequent elimination of *molecular* hydrogen via transition structure **28** to produce $CH_2O^{\bullet+}$ (**13**). In the absence of complex **5**, the reaction $CH_2OH_2^{\bullet+}$ (**3**) → CH_2OH^+ (**9**) + H$^{\bullet}$ → $CH_2O^{\bullet+}$ (**13**) + 2H$^{\bullet}$ would produce formaldehyde cation plus *atomic* hydrogen at an additional energy cost of more than 400 kJ mol^{-1}!

(50) See, for example, McAdoo, D. J. *Mass Spectrom. Rev.* **1988**, *7*, 363.

Conclusions

Several important conclusions emerge from this study.

(a) G1 and G2 theory both perform well in describing rearrangement and dissociative reactions of the methanol radical cation, with G2 achieving an accuracy of better than 0.1 eV for stable structures and 0.15 eV for transition structures for most of the energy comparisons presented in this paper. In the small number of cases where the difference between theoretical and experimental relative energies is greater than 0.15 eV, there are grounds for questioning the experimental values.

(b) The good agreement between theory and experiment for comparisons involving transition structures is very encouraging, but it should be noted that the number and types of systems examined have been limited, and the experimental results are often associated with considerable uncertainties. Further study is required to assess the generality of the results obtained here.

(c) The calculations indicate that many fragmentation reactions have substantial reverse activation energies and these need to be taken into account in deriving heats of formation from appearance energy measurements.

(d) The calculations indicate that the effect on appearance energies of isotopic substitution can be significant, e.g., 0.17 eV for the threshold production of HCO^+ from CD_3OH, and these should also be taken into account in deriving thermochemical information.

(e) The calculations reveal four distinct pathways for the production of HCO^+ (**19**) from CH_3OH (**1**). The agreement between calculated energies for these pathways and experimental appearance energies is quite striking.

(f) The comparisons presented here support the recent revision of the $\Delta H_f°_{298}$ value for $HCOH^{\bullet+}$ (**14**) to 968 kJ mol^{-1} and suggest that a reexamination of the $\Delta H_f°_{298}$ value for COH^+ (**20**) may also be appropriate. Good agreement between theory and experiment for the three independent comparisons involving COH^+ is achieved for a $\Delta H_f°_{298}$ value for COH^+ of 983 kJ mol^{-1}.

(g) Involvement of ion–neutral complexes can result in dramatically reduced reaction barriers.

Acknowledgment. We gratefully acknowledge a generous allocation of time on the Fujitsu FACOM VP-100 of the Australian National University Supercomputer Facility and the award of a Visiting Fellowship (to J.A.P.) by the Research School of Chemistry, Australian National University. Part of this work was carried out under NSF Grant CHEM-89-18623.

Registry No. 1, 67-56-1; **2**, 12538-91-9; **3**, 110596-50-4; **9**, 17691-31-5; **12**, 50-00-0; **13**, 54288-05-0; **14**, 135395-06-1; **18**, 2597-44-6; **19**, 17030-74-9; **20**, 60528-75-8; **21**, 630-08-0; **22**, 135501-39-2; **38**, 12385-13-6.